

## MICROSCOPY AND SURFACE ROUGHNESS AT END-MILLING OF OL37 STEEL

Cristina Ileana PASCU, Iulian POPESCU

University of Craiova, Romania

**Abstract.** In this paper a study, based on a factorial experiment, microscopy and surface roughness results in milling steel cylinder front-OL37 is presented.

Variable parameters in the experiment were: cutting speed, feed rate and depth of cut. The levels of these variables and the experimental program are presented. The kinematics of cutting for milling operation has been studied, demonstrating that is a rolling motion with gliding, the blade point trajectories are modified orthocycloides. Surface roughness results on two perpendicular directions: longitudinal and transverse has been measured. Modern equipment used allowed values for Ra, Rz, Rq on both directions.

Values factorial experiment results were tabulated, and after processing nonlinear relationships were obtained for the parameter Ra. Microscopic images and diagrams of the surface roughness are presented. Also, relationships for roughness have been established.

**Keywords:** steel milling, roughness, microscopy, milled surfaces.

### 1. Introduction

Milling of different materials with different mills, including end-milling cutter has been studied over time in different aspects.

Were studied and Chips and surface roughness resulted after milling have been studied, following such complex phenomena on the cutting area and from the contact surface tool-chip-piece. Sections chips are also measures of these phenomena.

In [1] the results on the milling cutting process are shown, detailing the flaws that may occur. Similar data are presented more detailed in [2].

In [3] are studied different aspects of milling with tools based on silicon carbide aiming different deposition regimes on the cutting edge, measuring the forces and temperature.

In [4] is simulated the milling process, step by step, establishing the forces, roughness and depositions on the cutting edge.

In [5] is established a mathematical model for milling process with helical milling n, settling reference systems mathematically correlated.

Take into account the vibration process, cutting forces and roughness.

In [6] is presented studied a procedure of assessing of the quality surface by nanoscale topography, establishing new concepts for microstructure of processed surfaces.

Other aspects are given in [7, 8, 9].

### 2. Experimental procedure

Factorial experiment was conducted with 15 samples, by executing end-millings on a piece of OL37 steel. On the four-side piece milling areas were delineated (figure 1). One channel on each area on one side has been milled, and then the piece has been rotated and has been milled areas on a new side and so on.

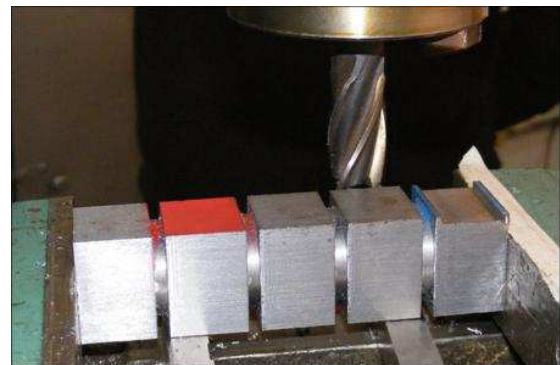


Figure 1. Experimental procedure

Milling cutter passed on the part edge, milling being complete. Milling was done on a vertical milling machine.

Although milling was end-milling type, the front surface only interested, like the final surface, because the cylinder area turned into chips.

In some areas that were to be mill network and squares networks have been plotted and other

surfaces were painted in different colors to be able to track the formation of chips and splinters, and to know the exterior surfaces of resulted chips.

Chip formation and flow was monitored using an image acquisition and analysis system – SIMI Motion, (SIMI Reality Motion Systems GmbH).

The system consists of an ultra-fast camera Panasonic, and Acer - Aspire 3000 Series. The

software allowed for the separation of each frame of one second of film.

The tool used was an end-milling cutter from high-speed steel, with  $D = 20$  mm diameter, given in figure 2.

The angles of adjustment were  $r = 1250$ ,  $r' = 50$ . Helix angle was 200, normal front rake was 120, and angle of clearance was 60.



Figure 2. End-milling cutter used

Levels of variables are given in table 1.

In table 2 the experimental program is presented. Details are presented in [10].

Table 1. Levels of variables

Parameters		Levels				
Real	Encoded	-2	-1	0	1	2
$n$ , rot/min	$x_1$	200	315	400	500	630
$v_f$ , mm/min	$x_2$	10	12.5	16	20	25
$a_p$ , mm	$x_3$	0.25	0.5	1	1.5	2

Table 2. Experimental program

Sample	Speed $n$ , rot/min	Cutting feed $v_f$ , mm/min	Cutting depth $a_p$ , mm	Cutting speed $v$ , m/min
1	315	12.5	0.5	20
2	500	12.5	0.5	31.4
3	315	20	0.5	20
4	500	20	0.5	31.4
5	315	12.5	1.5	20
6	500	12.5	1.5	31.4
7	315	20	1.5	20
8	500	20	1.5	31.4
9	200	16	1	12.5
10	630	16	1	40
11	400	10	1	25
12	400	25	1	25
13	400	16	0.25	25
14	400	16	2	25
15	400	16	1	25

For cutting depth quotation  $a_p$ , the point at the maximum distance from the finished surface has

been considered. The cutting feed  $v_t$  was in mm/min, speed  $n$  in rot/min, cutting depth  $a_p$  in mm and cutting speed in m/min.

### 3. Kinematics of milling. Development with or without gliding

In the figure 3 is shown the manner of generation for an orthocycloide by point E, rolling circle having  $AM = r$  radius.

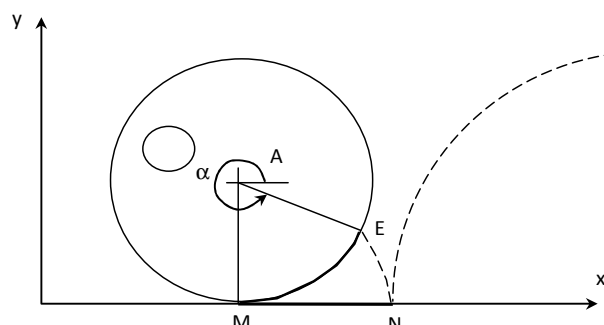


Figure 3. Development with gliding

In circle with  $r$  radius rolling without gliding on x-axis, then EM sector is equal with MN segment (figure 3) so can be describe coordinates equations of E point:

$$x_E = S_0 + a \cdot \cos(270^\circ - \alpha) \quad (1)$$

$$y_E = r + a \cdot \sin(270^\circ - \alpha) \quad (2)$$

The resulted curve, the trajectory of E, is an orthocycloide as in figure 4, resulting in  $r = 30$  mm, for two complete rotations, drawn with the equations above. Two branches of orthocycloide resulted.



Figure 4. Resulted orthocycloide

Same orthocycloide is obtained if it is considers cutting and feed motions as independent movements, but taking the calculated feed so that for a complete rotation of the circle, the space covered is equal with the length of the circle:

$$x = 2\pi \cdot r \cdot \frac{\alpha^\circ}{360^\circ} \quad (3)$$

Since the two orthocycloids overlap, for figure visualization, the actual displacement is considered equal to 0.8 theoretical displacements; in this case obtain a curve like orthocycloide modified loop and for this time there are rolling bearings **with gliding**.

In figure 5 a normal and altered states orthocycloide is presented.



Figure 5. A normal and altered orthocycloide

At milling, in a minute can be executed “*n*” rotations, and the feed is *f* mm, which means that for a rotation the movement is *f/n* mm/rot. If for a rotation of 36° degrees the motion is *f/n* mm, then for rotation angle  $\alpha$  results a movement of  $\alpha_f / (n \cdot 360)$ .

For example it was considered  $n = 1, f = 20$  mm and the resulting curve was an altered state orthocycloide, with gliding, shown in figure 6, which is different than a normal orthocycloide.

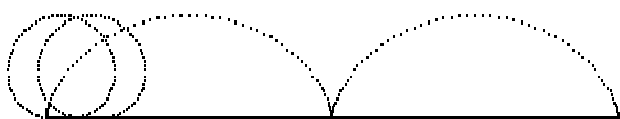


Figure 6. Curve altered state orthocycloide

After several tests with different regimes, the following can be establishing:

- with feed increasing the pace between generating circles centers growth;
- with rotative speed increasing is reduced the pace between of generating circles;
- different combinations of *n* and *f* provide different steps between the circles centers generating.

From the above results the following conclusions:

- commonly used speeds and feeds in end-milling ensures good "sweeping" of generated area;
- there are an infinity of points on each edge and more edged, generated curves are very dense, so the geometric roughness it is very good;
- curves generated from this milling it appears modified orthocycloides because are rolling bearings **with gliding**.

#### 4. Directions of roughness measurement

The figure 7 shows that, geometrically, roughnesses are different values in different areas of the machined surface. Cutter chips from the right side to the left.

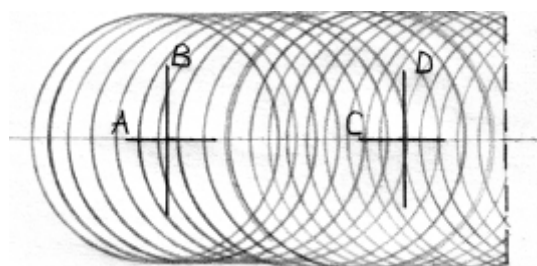


Figure 7. End-mill direction

It appears that after the direction C in this area, finished surface has edged past both the chip and those who were in the passive course and only smooth the surface. On A direction they past only edged from the active period, so there was not a smooth. It also notes that for the lines B, D, arcs of circles cut on these directions are different from those on lines A, C.

The roughness values are given as below:

- end-wise, namely on C direction;
- on crosswise direction, namely the D direction.

#### 5. Experimental results

Milled surfaces were studied under a microscope Handheld Digital model # 44300, Roughness was measured on each level with a roughness to touch type Mitutoyo, Japan, model SJ-201P. For each sample was measured roughness after two directions: one in the feed direction (longitudinal line C in figure 7) and the other as the direction perpendicular to the direction of feed (cross line D in figure 7). Roughnesses after the two directions are different because the first measure the radius of the circle direction (parallel to feed direction) and the other on a subtense of the rounding of the considered circle. Microscope images obtained appear identical, but they are different due to plastic deformation variables used cutting regimes. All surfaces are clear traces

processed cutter teeth, so it can be clearly observed that traces in the form of semicircles face in the speed of feed. It should be noted that there are whole circles just half circles, which is mainly explained by the fact that cut edge only in the area in front, where they are chip, and after covered the arch of 180°, reached in the back where it already arcs are formed and the main cutting edge is no longer the chip. In this area, the main cutting edge is pushed and to track (the cutter teeth being inclined, there is a component of cutting force to the bottom), so there is a small elastic deformation of the tool which is pressed and pushed out in front of the back, namely is increased by degree fraction given part surface.

Therefore there are no circles mainly which means that on the rear area the main cutting edge cut not. Side cutting edge meets some small irregularities that chips away, but this resulted only at measuring of the roughness.

For sample 1 the image from figure 8 has been obtained.

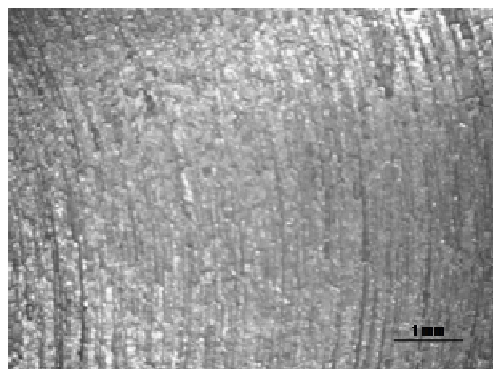


Figure 8. Resulted surface for sample 1

From the figure 8 can be observed arcs on feed direction, and, also, some deeper channels and scales on the final surface.

In figures 9 and 10 resulted micro-unevenness are shown (in figure 9 longitudinal roughness and in figure 10 the crosswise roughness).

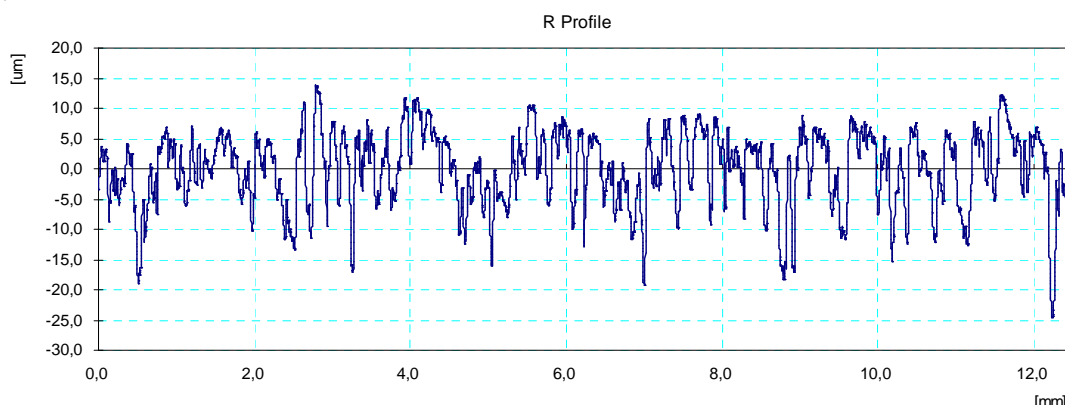


Figure 9. Longitudinal roughness for sample

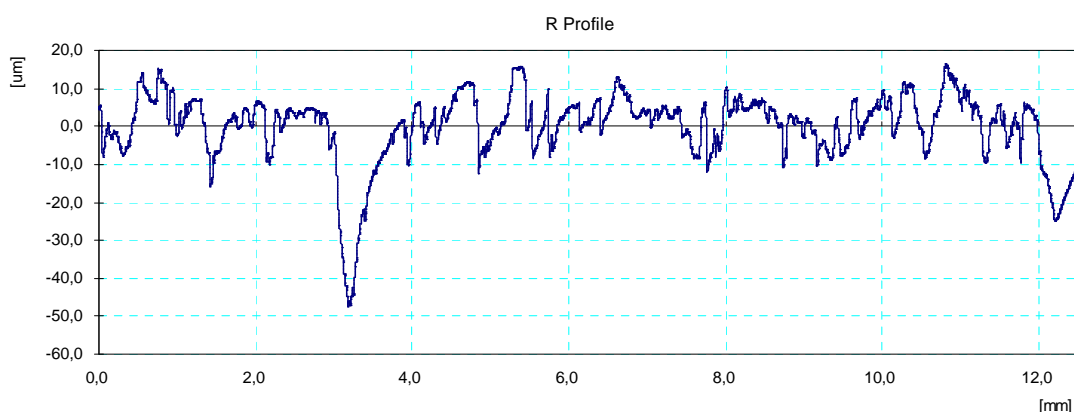


Figure 10. Crosswise roughness for sample 1

Next will be presented only the longitudinal roughness.

It can be noted that the prominences and holes in crosswise direction are higher than those of the longitudinal direction, a trend that occurs over the

next samples.

For sample 2, the profile appears in figure 11.

Surface microscopy shows a good consistency, the scales are rare, but there are deposits on the edge, stuck on the track.

Cutting speed is:  $v = \pi \cdot 20 \cdot 500 / 1000 = 31.4$  m/min, a speed that is still occurring deposits on the cutting edge at chip removing process of OL37

steel. They worked without cooling fluid. Compared with a sample 1, here protrusions and holes are smaller.

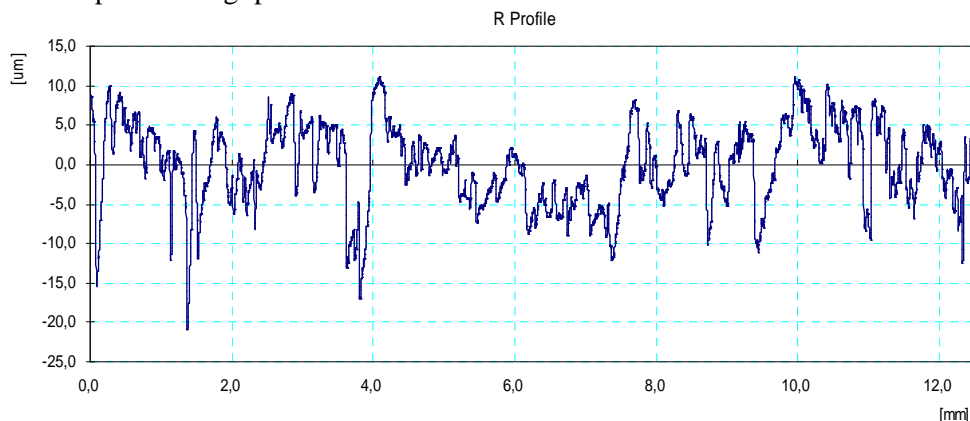


Figure 11. The profile of sample 2

For sample 3, compared with sample 1 only the feed has been increased, so that the resulting surface has larger steps between the arcs of circles and more fractures. Micro-unevenness's shown in figure 12, being smaller than those of sample 1, which

show that small feeds are not provide always a better surface roughness, interfering with plastic deformations.

In figure 13 the micro-asperities for sample 4 are presented.

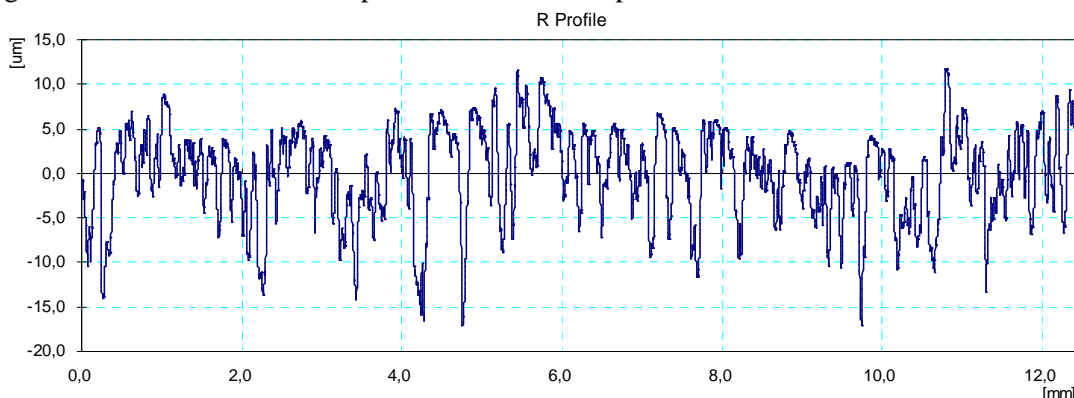


Figure 12. Micro-unevenness's of sample 3

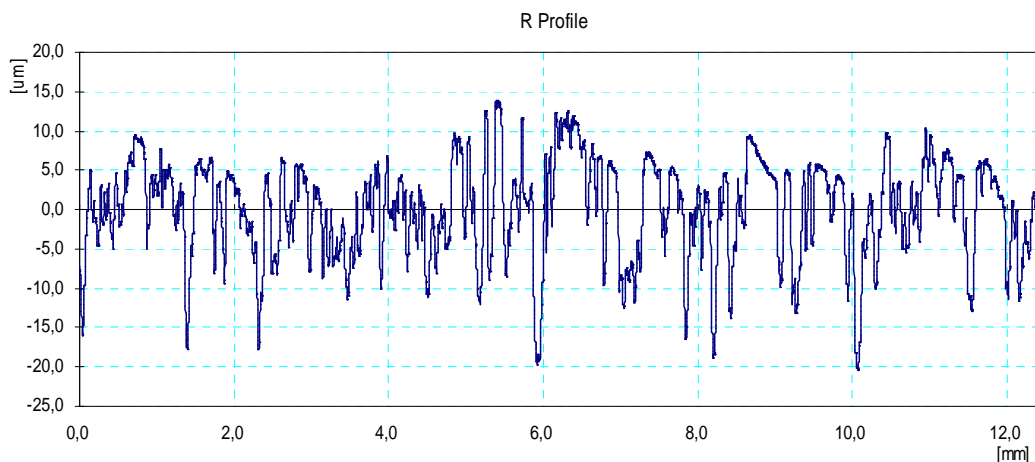


Figure 13. Micro-unevenness's of sample 4

For reasons of space is still only give some pictures so:

- figures 14 and 15 for sample 5;
- figures 16 and 17 for sample 7.

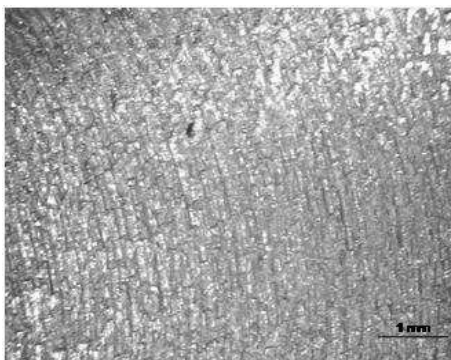


Figure 14. Resulted surface for sample 5

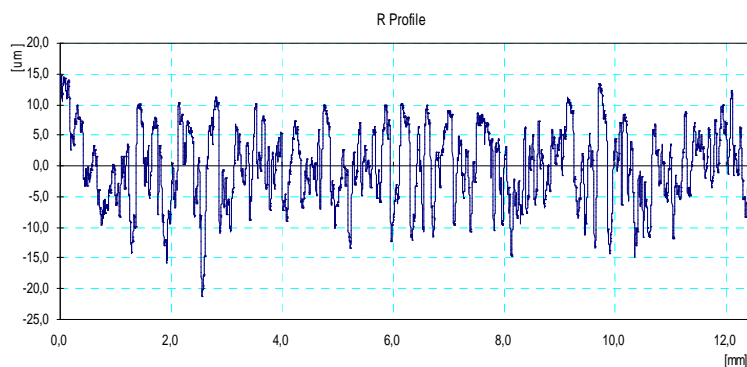


Figure 15. Micro-unevenness's of sample 5

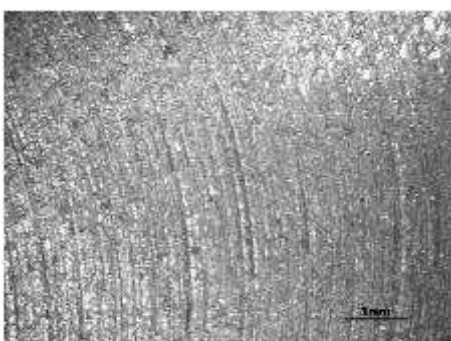


Figure 16. Resulted surface for sample 6

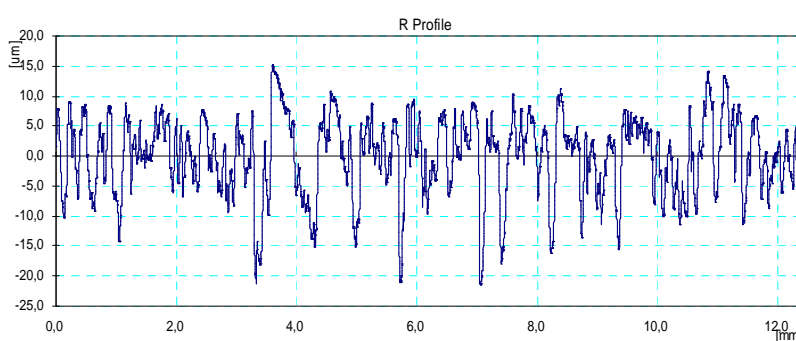


Figure 17. Micro-unevenness's of sample 6

## 6. Diagrams and relationships

The obtained values of final roughness parameters for each of 15 samples are summarized

in table 3. These values have been processed, resulting in relationships and data tables below.

Table 3. The obtained values of final roughness parameters

Sample	Ra longitudinal	Rz crosswise	Rq longitudinal	Ra crosswise	Rz crosswise	Rq crosswise
1	4.99	30.13	6.2	6.36	35.73	8.45
2	5.08	29.33	6.38	4.29	24.07	5.23
3	4.13	23.33	5.14	4.17	25.47	5.26
4	5	28.17	6.18	4.76	23.68	5.76
5	5.04	28.37	6.12	5.53	30	6.78
6	5.19	29.62	6.34	6.07	35.03	7.65
7	5.28	29.7	6.55	4.83	27.07	6.1
8	4.86	28.51	6.14	4.04	23.8	5.19
9	4.8	28.34	5.82	4.19	27.13	5.5
10	5.73	29.61	6.85	8.73	45.76	11.41
11	6.12	36.47	8.08	8.4	44.3	10.94
12	3.46	21.54	4.31	3.94	23.22	4.95
13	8.33	50.32	10.84	7.18	39.08	9.54
14	5.41	31.27	6.59	5.04	29.24	6.22
15	4.77	30.26	6.05	4.52	23.32	5.43

In table 4 the values obtained for  $Ra$  at longitudinal measuring with cutting regimes used are presented. Also, the  $Ra$  value, calculated with relation resulted after factorial experiment, are presented.

The obtained relationship is following [11]:

$$\begin{aligned}
 R_{along} = & 5.901917 + (5.274773 \cdot 10^{-2})v + \\
 & + (.1346359)v_f + (-3.756226)a_p + \\
 & + (1.70451 \cdot 10^{-3})v \cdot v_f + (-3.958228 \cdot 10^{-2})v \cdot a_p + \quad (4) \\
 & + (7.366055 \cdot 10^{-2})v_f \cdot a_p + (-3.040433 \cdot 10^{-4})v^2 + \\
 & + (-0.48851 \cdot 10^{-2})v_f^2 + (1.454742)a_p^2
 \end{aligned}$$

Table 4. The values obtained for  $Ra$  at longitudinal measuring

Sample	$v$	$v_f$	$a_p$	$Ra$ calculated	$Ra$ measured
1	19.79202	12.5	.5	5.84686	4.99
2	31.4159	12.5	0.5	6.29663	5.08
3	19.79202	20	0.5	4.8293	4.13
4	31.4159	20	0.5	5.427667	5
5	19.79202	12.5	1.5	5.137462	5.04
6	31.4159	12.5	1.5	5.127133	5.19
7	19.79202	20	1.5	4.672356	5.28
8	31.4159	20	1.5	4.810624	4.86
9	12.56636	16	1	4.70826	4.8
10	39.58404	16	1	5.372398	5.73
11	25.13272	10	1	5.201771	6.12
12	25.13272	25	1	3.462335	3.46
13	25.13272	16	0.25	6.387905	8.33
14	25.13272	16	2	5.864136	5.41
15	25.13272	16	1	5.072376	4.77

For  $Ra$ , after crosswise direction measuring, following relationships are obtained:

$$\begin{aligned}
 R_{atransv} = & 23.64966 + (-.55511)v + \\
 & + (-.119633)v_f + (-3.338806)a_p + \\
 & + (6.884016 \cdot 10^{-3})v \cdot v_f + (.062448)v \cdot a_p + \\
 & + (-5.519098 \cdot 10^{-2})v_f \cdot a_p + (8.904338 \cdot 10^{-3})v^2 + \\
 & + (2.318275 \cdot 10^{-2})v_f^2 + (1.9087753)a_p^2
 \end{aligned} \quad (5)$$

### 7. Conclusions

At milling, between cutting tool and piece is produced a development with gliding.

Longitudinal roughness is smaller than the crosswise roughness.

Microscopy of measured surfaces shows symmetrical flaws and for some cutting regimes crushed deposits on the cutting edge of bit are observed.

Nonlinear relationships were determined for the roughness resulted after end-milling of OL37 steel.

### References

1. \*\*\**Milling Process, Defect, Equipment*. Available from: <http://www.custompartnet.com/wu/milling>, Accessed:03/04/2011
2. \*\*\**Metal Cutting Processes 2 – Milling*. Available from: <http://mmu.ic.polyu.edu.hk/handout/0103/0103.htm>. Accessed: 04/04/2011
3. Elbestawi, M.A., Di Yang, Di, Min Tan, Elwardany, T., (1993) *Performance of whisker-reinforced ceramic tools in milling nickel-based super alloy*. CIRP Annals, STC C, Vol. 42, No. 1, p. 99-112, ISSN: 0007-8506
4. Smith, S., Tlustý, Y., (2003) *Efficient simulation programs for chatter in milling*. CIRP Annals, STC M, Vol. 42, No. 1, p. 463-472, ISSN: 0007-8506
5. Altintas, Y., Engin, S., (2001) *Generalized Modeling of Mechanics and Dynamics of Milling Cutters*. CIRP Annals,

6. Jiang, X., Scott, D., Whitehouse, M., (2007) *Freeform Surface Characterisation - A Fresh Strategy*. CIRP Annals, STC S, Vol. 56, No. 1, p. 553-547, ISSN: 0007-8506
7. Bouzakis, K.D., Aichouh, P., Efstathou, K., (2003) *Determination of the chip geometry, cutting force and roughness in free form surfaces finishing milling, with ball end tools*. International Journal of Machine Tools & Manufacture, Vol. 43, p. 499-514, ISSN 0890-6955
8. Davies, M.A., Burns, T.J., Evans, C.J., (1997) *On the dynamics of chip formation in machining hard metals*. Annals of the CIRP, Vol. 46, No. 1, p. 25-30, ISSN: 0007-8506
9. Wang, M.Y., Chang, H.Y., (2004) *Experimental study of surface roughness in slot end milling AL2014-T6*. International Journal of Machine Tools & Manufacture, Vol. 44, p. 51-57, ISSN 0890-6955
10. Popescu, I., (1987) *Optimizarea procesului de aşchiere (Optimization of Cutting Process)*. „Scrisul Romanesc” Publishing House, Craiova, Romania (in Romanian)
11. Pascu, I.C., Popescu, I., (2010) *Precizie și rugozitate. Aplicații pentru procesul de frezare (Precision and Roughness. Applications at Milling Process)*. Sitech Publishing House, ISBN 978-606-11-0745-2, Craiova, Romania (in Romanian)